



Biopolymers

**MESOSCOPIC STRUCTURE OF PECTIN IN SOLUTION**

Journal:	<i>Biopolymers</i>
Manuscript ID	BIP-2016-0181.R1
Wiley - Manuscript type:	Original Article
Date Submitted by the Author:	n/a
Complete List of Authors:	Alba, Katerina; University of Huddersfield, Biological Sciences Bingham, Richard; University of Huddersfield, Biological Sciences Kontogiorgos, Vassilis; University of Huddersfield, Biological Sciences
Keywords:	pectin, SAXS, polyelectrolyte, polysaccharide

SCHOLARONE™  
Manuscripts

1  
2  
3  
4  
5  
6  
7  
8  
9  
10  
11  
12  
13  
14  
15  
16  
17  
18  
19  
20  
21  
22  
23  
24  
25  
26  
27  
28  
29  
30  
31  
32  
33  
34  
35  
36  
37  
38  
39  
40  
41  
42  
43  
44  
45  
46  
47  
48  
49  
50  
51  
52  
53  
54  
55  
56  
57  
58  
59  
60

1  
2  
3  
4  
5  
6  
7  
8  
9  
10  
11  
12  
13  
14  
15  
16  
17

**MESOSCOPIC STRUCTURE OF PECTIN IN SOLUTION**

K. Alba, R. J. Bingham, V. Kontogiorgos\*

Department of Biological Sciences, University of Huddersfield, HD1 3DH, UK

\*Corresponding author

Tel: 0044 -1484-472488.

e-mail address: v.kontogiorgos@hud.ac.uk

1  
2  
3 18 **Abstract**  
4  
5 19

6 20 Mesoscopic structure of pectin with different molecular characteristics was investigated by  
7  
8  
9 21 means of small angle X-ray scattering (SAXS), electrokinetic measurements and data  
10  
11 22 modelling. The influence of a broad range of pH (2-7) on chain conformation in the dilute  
12  
13 23 and semi-diluted regime was investigated. Scattering data and concomitant analysis revealed  
14  
15 24 two length scales at all environmental conditions studied. pH showed greater influence at  
16  
17 25 acidic values (pH 2.0) enhancing the globular component of the structure due to association  
18  
19 26 of galacturonic acid residues. Double logarithmic scattering intensity plots revealed fractal  
20  
21 27 dimensions of  $1.9 \pm 0.2$  in the low- $q$  regime and  $1.5 \pm 0.2$  in the high  $q$ -region, **irrespectively**  
22  
23 28 **of** the specific environment. Increase in branching of RG-I regions of the polysaccharide  
24  
25 29 chains enhanced the compact conformation irrespectively of the pH or concentration. The  
26  
27 30 present work shows that radical changes in pectin conformation can be induced only under  
28  
29 31 strongly acidic conditions a finding that has important consequences in tailoring the  
30  
31 32 technological performance of these biopolymers.  
32  
33  
34  
35  
36  
37

38

39 34 **Keywords:** pectin, SAXS, polyelectrolyte, polysaccharide  
40  
41  
42  
43  
44  
45  
46  
47  
48  
49  
50  
51  
52  
53  
54  
55  
56  
57  
58  
59  
60

35

36

37

38

39

40

41

42

43

44

## 1. Introduction

The solution conformation of polysaccharides plays a determinant role in their functional properties. The first stage that is involved aqueous dispersion of biopolymers is hydration of the chains and exposure of the functional groups (e.g., hydroxyl, carboxyl, methyl, acetyl etc.). This is followed by interactions between the chains at the molecular level that lead to either self-association (i.e., aggregation) or heterotypic cooperation among different chains. The latter results in formation of three-dimensional structures (i.e., gels), biopolymer-biopolymer complexes or highly entangled viscous solutions. Mechanical properties and functional performance can be in most cases easily adjusted and the mechanistic underpinnings between the surrounding environment (e.g., pH, ionic strength, presence of cross linkers etc.) and chain behaviour are well understood.<sup>1</sup>

Pectin is a heteropolysaccharide of particular industrial importance (e.g., food and pharmaceutical industries) with diverse functionality due to its tunable primary structure. It is a diblock copolymer primarily consisting of homogalacturonan (HG) and rhamnogalacturonan I (RG-I) and the fine structure and functionalization of these two blocks control the properties of the biopolymer (Figure 1). Other moieties may be observed depending on the botanical origin and method of extraction such as rhamnogalacturonan II (RG-II), arabinogalactan, arabinan, apiogalacturonan and xylogalacturonan.<sup>2</sup> Proteins may also be attached to side chains of RG-I regions further contributing to the complexity of the structure (Figure 1). The presence of galacturonic acid residues (D-GalA) causes pectin to become negatively charged at neutral pH making it essentially an anionic polyelectrolyte. In addition, D-GalA residues are frequently methyl esterified yielding a range of pectins with different degree of methyl esterification. Typically, pectins with degree of methyl-esterification greater than 50% are described as high methyl-esterified (HM) and those with

1  
2  
3 70 lower than 50% are defined as low methyl-esterified (LM). *O*-Acetylation is also possible  
4  
5 71 that usually occurs at the *O*-2 or *O*-3 position of rhamnose (Rha) or of D-GalA (Figure 1).  
6  
7 72 The degree of methylation (DM) and acetylation (DA), in turn, may also influence  
8  
9 73 conformational characteristics *via* hydrophobic interactions between chains.  
10

11  
12 74 This characteristic (i.e., free or methyl esterified D-GalA) makes solution conformation  
13  
14 75 of pectin particularly responsive to the surroundings (e.g., ionic strength, pH, presence of  
15  
16 76 divalent cations etc.) and to the fine structure (e.g., methyl and acetyl groups, molecular  
17  
18 77 weight or branching). For that reason, the dispersion medium can be easily used to control  
19  
20 78 functionality, as for instance in gelation or arrangement at the oil-water interface. As  
21  
22 79 dispersion into an aqueous medium is always the first step towards a desired application,  
23  
24 80 understanding of conformations and how they are affected by the various factors is key for  
25  
26 81 tailoring pectin functionality. Previous small angle X-ray and neutron scattering and  
27  
28 82 molecular modelling work on solution conformation of pectin has highlighted the importance  
29  
30 83 of DM, rhamnose content, molecular weight<sup>3</sup> and HG/RG-I ratio<sup>4</sup> at neutral pH. However,  
31  
32 84 interplay between the above parameters and pH, which control the functionality, has been  
33  
34 85 largely disregarded. In the present investigation, therefore, we aim to unveil the relationships  
35  
36 86 between concentration, branching and solvent pH on the solution conformation of pectin.  
37  
38  
39  
40  
41

## 42 87 **2. Materials and Methods**

### 43 88 *2.1 Materials*

44  
45 89 Pectin from okra pods with a low degree of methyl esterification was isolated and  
46  
47 90 characterised as described elsewhere in detail.<sup>5</sup> Important chemical and physical  
48  
49 91 characteristics relevant to the present investigation are reproduced in Table S1 in  
50  
51 92 supplementary data. Samples were labelled as OP2 and OP6. Sodium chloride, citric and  
52  
53 93 phosphate salts for buffer solutions (100 mM) were obtained from Sigma Aldrich (Poole,  
54  
55 94 UK).  
56  
57  
58  
59  
60

## 95 2.2 Sample preparation

96 Okra pectin was dispersed at 0.1 or 1.0 g dL<sup>-1</sup> in 0.1 M buffers with pH 2.0, 4.0 (citric),  
97 6.0 and 7.0 (phosphate) in the presence of 0.1 M NaCl. Samples were left overnight under  
98 continuous stirring to ensure complete solubilisation. Following solubilisation, samples were  
99 centrifuged to remove any insoluble cellulosic oligomers and were subjected to SAXS  
100 measurements at room temperature, as described in the next section.

## 101 2.3 SAXS measurements

102 SAXS data were acquired using a Bruker Nanostar from pectin solutions in the  
103 presence of 0.1 M NaCl. Samples of about 100 µl were sealed in a 1.5 mm bore quartz glass  
104 capillary and the sample chamber was evacuated to minimize background scattering. The  
105 sample to detector distance was 106.85 cm. The  $q$ -axis and beam centre were calibrated using  
106 the scattering pattern of silver-behenate salt ( $d$ -spacing = 5.84 nm). The momentum transfer  
107 was defined as  $q = 4\pi\sin(\theta)/\lambda$  where  $\theta$  is the scattering angle and  $\lambda$  the X-ray beam  
108 wavelength. Each scattering data set consisted of 5 × 5000 s exposures. Scattering data were  
109 collected at all pH values above and below the critical overlap concentration of the  
110 biopolymers ( $c^*$ ) that demarcates the dilute from semi-dilute regimes of the biopolymers. For  
111 each sample, the equivalent scattering data collected for buffer (5 × 5000 s) was subtracted  
112 using the Primus software.<sup>6</sup>

## 113 2.4. SAXS data analysis

114 Data analysis was performed using the software Scatter (v. 2.3H, BIOISIS). Cross  
115 sectional radius of gyration ( $R_c$ ) was calculated using the Guinier approximation from the  
116 intermediate  $q$ -region so as  $q \times R_c < 1.4$ . Plots of  $q^2 \times I(q)$  versus  $q$  (Kratky plots) were also  
117 constructed to examine the influence of pH on the conformation of the macromolecules.  
118 Double logarithmic intensity plots were also constructed and the fractal dimensions were

1  
2  
3 119 calculated from the exponents of power law regime of the curves. The exponents were  
4  
5 120 calculated by fitting a power function of the form  $f(x) = cx^{d_f}$  where  $c$  is a constant and  $d_f$  is  
6  
7 121 the fractal dimension. The Ornstein-Zernike relationship was curve-fitted to the scattering  
8  
9  
10 122 intensity curves of semi-dilute solutions between 0.03 and 0.13  $\text{\AA}^{-1}$ . Non-linear regression of  
11  
12 123 data (curve fitting) was performed using Prism v.6 (Graphpad Software, SanDiego, USA).

13  
14  
15 124

### 17 125 3. Results and Discussion

18  
19  
20 126 Figure 2 shows typical small-angle X-ray scattering intensity plots of pectin samples at  
21  
22 127 all pH values in the presence of 0.1 M NaCl in the dilute (Fig 2a) and semi- dilute regime  
23  
24 128 (Fig 2b) of the biopolymers. The screening from NaCl is required to prevent complexities  
25  
26 129 that may stem from changes in chain dimensions due to intra- and inter- molecular  
27  
28 130 electrostatic interactions.<sup>7</sup> In the presence of 0.1 M NaCl it is anticipated that the scattering  
29  
30 131 curves reflect the conformations of the chains without intermolecular electrostatic  
31  
32 132 interactions<sup>7-10</sup> and is a common practice in SAXS sample preparation of biological or  
33  
34 133 synthetic polyelectrolytes.<sup>3,11,12</sup> It should be mentioned that it is possible to observe  
35  
36 134 broadening of the scattering intensity curves at concentrations greater than the critical  
37  
38 135 concentration ( $c^*$ ) of the biopolymers.<sup>13</sup> Nevertheless, the overall shape of the curves remains  
39  
40 136 unaltered indicating negligible intermolecular interaction and no conformational changes at  
41  
42 137 the concentrations studied. Additionally, NaCl provides adequate screening, as at low  $q$  no  
43  
44 138 evident electrostatic peak is observed in the scattering patterns, something that is common in  
45  
46 139 polyelectrolyte solutions in the absence of screening.<sup>14,15</sup> Although the shoulder at about 0.08  
47  
48 140  $\text{\AA}^{-1}$  could be related to the electrostatic peak or inter-backbone distances, electrostatic  
49  
50 141 interactions do not show measurable influence on the structure and the intermolecular  
51  
52 142 distance between pectin chains. As a result, the observed conformational changes can be  
53  
54 143 comfortably attributed to the influence of solution pH. The peak at about 0.22  $\text{\AA}^{-1}$  ( $\sim 29 \text{\AA}$ )

1  
2  
3 144 could be related to side-chain interchain distance i.e., to the distance between the branches of  
4  
5 145 RG-I units between different chains.  
6  
7

8 146 The scattering curves show marginal dependency on pH between 4 and 7 indicating that  
9  
10 147 chain conformation is not particularly affected in this range. pH-Depended structures start  
11  
12 148 developing by lowering pH below 4, an observation that is particularly evident in the semi  
13  
14 149 dilute regime of the biopolymers (Fig 2b). It should be mentioned that scattering intensity  
15  
16 150 increases for all samples in the semi dilute region because the number of scattering particles  
17  
18 151 in the scattering volume increases with increasing concentration.  $\zeta$ -Potential titration between  
19  
20 152 pH 1.0 and 9.0 (Figure S1, supplementary data) reveal that below pH 4 there is a sharp  
21  
22 153 decrease in biopolymer charge due protonation of the carboxyl groups of the galacturonic  
23  
24 154 acid residues. At pH 2.0 biopolymer coils of both samples are almost devoid of charge ( $\sim -4$   
25  
26 155 mV) resulting in reduction in the strength of intramolecular interactions. The uniform  
27  
28 156 decrease of the entire scattering intensity curve at pH 2.0 indicates that pH-dependent  
29  
30 157 changes have been brought about in the pectin chains in the entire range of measured length  
31  
32 158 scales. At limited electrostatic repulsions at pH 2, the compact conformations result in an  
33  
34 159 overall reduction of total scattering intensity of both samples (Figure 2 and Figure 2b inset).  
35  
36 160 This is expected, as scattering is proportional to the square of the particle volume and  
37  
38 161 additional contributions may also be present from changes in scattering contrast.<sup>16</sup> It can be  
39  
40 162 seen (Figure 2b vs. Figure 2b inset) that sample OP2 exhibits greater changes in scattering  
41  
42 163 intensity with pH than OP6 demonstrating that acidic environments induce greater  
43  
44 164 conformational modifications in this sample. OP6 higher scattering intensity is partially  
45  
46 165 ascribed to the greater content of RG-I regions, as it will be discussed below in detail.  
47  
48 166 Congruent results have been also reported for LM-pectin and chitosan solutions at different  
49  
50 167 temperatures and concentrations.<sup>17</sup>  
51  
52  
53  
54  
55  
56  
57  
58  
59  
60



1  
2  
3 168 To further evaluate the influence of pH on the degree of disorder plots of  $q^2I(q)$  vs.  $q$   
4  
5 169 (Kratky plots) were constructed (Figure 3). Curves show a distinct peak at about  $0.07 \text{ \AA}^{-1}$   
6  
7 170 followed by a sharp decay before starting increasing again at  $0.15 \text{ \AA}^{-1}$ . Such a curve-shape is  
8  
9 171 typical of partially folded chains with elongated domains corresponding to multidomain  
10  
11 172 particles<sup>18</sup> indicating that pectin samples consist of regions with partially folded and extended  
12  
13 173 conformations. This is also a common observation in multi-domain proteins, where flexible  
14  
15 174 linkers connect two or more globular domains, resulting in Kratky plots with contributions  
16  
17 175 from both of these structurally discrete regions.<sup>19</sup> Peaks at  $0.07 \text{ \AA}^{-1}$  have been previously  
18  
19 176 observed for samples with multidomain structures<sup>20</sup> whereas the peak that occurs at about  
20  
21 177  $0.21 \text{ \AA}^{-1}$  has been attributed in cinerean solutions to the presence of rod-like structures.<sup>21</sup> The  
22  
23 178 dual nature in the conformations of pectin particles seems to be preserved irrespectively of  
24  
25 179 the pH values. It is difficult to assess quantitatively the extent to which pH affects  
26  
27 180 conformations at this stage, however, qualitative inspection of Kratky plots show that peaks  
28  
29 181 at  $0.07 \text{ \AA}^{-1}$ , that indicate folded structures, become more prominent at low pH. These plots  
30  
31 182 are recognizably different from Kratky plots that have been reported in the literature for  $\lambda$ -  
32  
33 183 carrageenan and fucoidan in 0.5 M NaCl,<sup>11</sup> soy soluble polysaccharides,<sup>22</sup> carboxymethyl  
34  
35 184 cellulose<sup>23</sup> or bacterial exo-polysaccharides<sup>24</sup> where chains adopt extended conformations  
36  
37 185 without pronounced peaks. It appears that the prominence of neutral sugar RG-I branches in  
38  
39 186 both samples (Table 1S, supplementary data), which is not influenced by changes in pH,  
40  
41 187 serves as the basis for the compact conformation, as it is preserved at all pH values. This is in  
42  
43 188 agreement with previous reports on the solution conformations of sugar beet pectin that  
44  
45 189 revealed that fractions rich in RG-I regions are more compact than those rich in HG regions.  
46  
47 190 <sup>4,25</sup> Additionally, the hydrophobic focal points of the chains (i.e., methyl and acetyl groups)  
48  
49 191 should contribute to the folding of the chains *via* hydrophobic interactions. OP2 samples are  
50  
51 192 overall more hydrophobic than OP6 but a clear link between hydrophobicity and  
52  
53  
54  
55  
56  
57  
58  
59  
60

1  
2  
3 193 conformation cannot be distinguished at this stage. The multidomain character of the sample  
4  
5 194 can be also visualised by observation of the pair distance distribution functions of the samples  
6  
7 195 (Figure S2, supplementary data).  
8  
9

10 The Guinier approximation can be used to describe the scattering from samples that are  
11  
12 asymmetric or elongated such that:  
13

14  
15  
16 198 
$$qI(q) \approx e^{-\frac{q^2 R_c^2}{2}} \quad (1)$$
  
17  
18

19 where  $R_c$  is the cross-sectional radius of gyration. Plots of  $\ln(qI)$  vs.  $q^2$  (Figure 2a, inset) yield  
20 the cross-sectional radius of gyration in the limit of  $qR_c < 1.4$  (Table 1). All samples show a  
21 rise in the low  $q$ -values deviating from rod-like structures confirming that samples have  
22 several domains that is frequently observed in biological polyelectrolytes in solution.<sup>11,26</sup> On  
23 first inspection, all values of  $R_c$  (Table 1) range between 12-24 Å irrespectively of the pH of  
24 the solvent. Closer examination reveals that  $R_c$  has a tendency to decrease with the  
25 differences being more dramatic between pH 7.0 and pH 2.0. With decrease of pH the HG-  
26 pectin moieties fold as ionization of carboxyl groups decreases. On the contrary, high pH  
27 values result in extended conformations. At this pH,  $R_c$  is greater due to the exposure of the  
28 branched RG-I regions. This is indeed the case, as sample OP6 has larger  $R_c$  than OP2, as it  
29 has a greater molar ratio of RG-I regions although the higher molecular weight could also  
30 contribute (Table 1S, supplementary data). The  $R_c$  values are generally higher but comparable  
31 to other polysaccharides in solution reflecting the presence of bulky side chains.<sup>11,26-28</sup>  
32  
33  
34  
35  
36  
37  
38  
39  
40  
41  
42  
43  
44  
45  
46  
47  
48

49 Double logarithmic plots of  $I(q)$  vs.  $q$  (Porod plots) can be used to provide information  
50 on the structural levels that are present in biopolymer coils and give a first insight to the  
51 conformation of the chains (Figure 4). Curves confirmed the two distinct length scales that  
52 are particularly evident in the samples above the  $c^*$  of the coils (Figure 4b) with a transition  
53 occurring at  $0.08 \text{ \AA}^{-1}$ . By fitting power law functions such as:  
54  
55  
56  
57  
58  
59  
60

1  
2  
3 217 
$$I(q) \sim I_0 q^{-d_f} \quad (3)$$
  
4  
5

6 218 is possible to calculate the fractal dimensions of the coils from the exponent of equation 3  
7  
8 219 (Table 1). In the fractal regime the structure of the coils is independent of the length scale of  
9  
10 220 observation and in real systems the self-similarity eventually terminates.<sup>29</sup> The two length-  
11  
12 221 scales that are present in the biopolymers under investigation hold until about 0.08 Å<sup>-1</sup> and  
13  
14 222 0.2 Å<sup>-1</sup>. Slope 1 fluctuates around -1.9 ±0.2 whereas slope 2 around -1.5 ±0.2 revealing  
15  
16 223 scattering from mass fractal particles. A fractal dimension of 2 describes a random walk,  
17  
18 224 while self-avoiding chains scale with exponent of 1.6. In terms of stiffness, random walk  
19  
20 225 chains are more flexible than self-avoiding chains indicating that pectin contains rigid and  
21  
22 226 flexible components in the structure. The first level of structure is related to the scattering of  
23  
24 227 the entire chain and is associated with the length scale of  $R_g$ . A transition from power law  
25  
26 228 with exponent -2 to -1.5 is related to the scattering of the second structural level which arises  
27  
28 229 from local structural subunits<sup>30</sup> that for the present system should correspond to the length of  
29  
30 230 the rod-like stiff structures. Mucins have shown similar behavior to the exponents with  
31  
32 231 changes in pH<sup>31</sup> whereas apple pectin that lacks side chains and the complexity of the present  
33  
34 232 samples has also revealed two length scales with slopes in the range of 2.1 and 1, for slopes 1  
35  
36 233 and 2, respectively.<sup>32</sup> Additionally, from the fractal exponents (Porod exponents) a first  
37  
38 234 insight into the shape of the molecules can be also obtained. For instance, flat oblate  
39  
40 235 ellipsoids have  $d_f = 2$  whereas random coils in good solvent have  $d_f = 5/3$  (1.6).<sup>33</sup> This is in  
41  
42 236 agreement with atomic force microscopy imaging of pectin preparations where the  
43  
44 237 macromolecular structures were described as "tadpoles"<sup>34</sup> containing two levels of distinct  
45  
46 238 structures (i.e., globular plus linear). In that work, the role of protein (~8%) has been  
47  
48 239 emphasized in the creation of these structures, which could also play a role to the structure  
49  
50 240 formation of the samples in the present investigation (~5% protein, Table S1). Additionally,  
51  
52 241 OP6 pectin shows marginally higher fractal dimensions than OP2, as a result of the more  
53  
54  
55  
56  
57  
58  
59  
60

1  
2  
3 242 extended branching of the chains (RG-I regions) that generally improve flexibility.<sup>4</sup>  
4  
5 243 Variations in pH do not particularly affect the slopes indicating little change in the length  
6  
7 244 scales of the macromolecules at all different conditions. The cross-sectional radius of  
8  
9 245 gyration for rod-like structures can be converted into a length scale, that corresponds to the  
10  
11 246 persistence length,  $l$ , of the constituent rods giving information about the stiffness of the  
12  
13 247 chains. From theoretical point of view, ideal random coils have persistence lengths equal to  
14  
15 248 zero whereas for extra-rigid rods it approaches infinity. In practice, the values range between  
16  
17 249 10-2000 Å for random coils (e.g. pullulan) or particularly rigid rods (e.g. DNA).<sup>35,36</sup> For  
18  
19 250 polyelectrolytes, the total persistence length  $l_{\text{tot}} = l_o + l_e$  is the sum of the persistence length of  
20  
21 251 the chain in the absence ( $l_o$ ) and presence ( $l_e$ ) of electrostatic interactions. Since the latter  
22  
23 252 interaction is screened by the high concentration of NaCl the chain dimensions will  
24  
25 253 correspond to  $l_o$ . For these systems, an approximate  $l_o$  can be calculated through the  $R_c$  of a  
26  
27 254 thin rigid rod, as  $l = \sqrt{12R_c^2}$  and was found to be between 38-83 Å (3.8-8.3 nm) (Table 1),  
28  
29 255 which is in close agreement with previously reported values (45-120 Å) indicating that pectin  
30  
31 256 samples attain semi-flexible conformations.<sup>3,4,25,36</sup> In accordance with the  $R_c$  values,  
32  
33 257 persistence length exhibits a step change between pH 7.0 and 2.0 due to folding of HG  
34  
35 258 regions at acidic conditions showing remarkable decrease in stiffness from the neutral pH. It  
36  
37 259 has been reported that increase in the RG-I domains leads to greater flexibility with  
38  
39 260 persistence length values in the range between 20-30 Å.<sup>4</sup> Persistence length of OP6 samples,  
40  
41 261 which are about 10% richer in RG-I domains than OP2 (Table 1S), are not in agreement with  
42  
43 262 the above generalization probably due to differences in the molecular weight and D-GalA  
44  
45 263 content. Finally, hydrophobicity (e.g., methyl and acetyl groups) is expected to play role in  
46  
47 264 the flexibility on the chains. Previous studies reporting estimates of persistence length as a  
48  
49 265 function of degree of methylation (DM) did not identify a clear relationship between DM and  
50  
51 266  $l_o$ .<sup>3</sup> In the present investigation, OP6 that is more hydrophobic displays a tendency to have  
52  
53  
54  
55  
56  
57  
58  
59  
60

1  
2  
3 267 greater persistence lengths than OP2 at all pH values showing that it attains relatively stiffer  
4  
5 268 conformations.  
6  
7

8 The scattering intensity from semi-dilute polymer solutions can be modeled using the  
9  
10 270 Ornstein-Zernike relationship as:<sup>37</sup>  
11

12  
13 271 
$$I(q) = \frac{I(0)}{1+q^2\xi^2} \quad (4)$$
  
14  
15

16  
17 272 where  $\xi$  is the correlation length of the chain and  $I(0)$  is the forward scattering intensity. At  
18

19 273 this juncture, it should be mentioned that for natural biopolymers is usually difficult to  
20

21 274 experimentally distinguish all three concentration regimes (i.e., dilute, semi-dilute ( $c^*$ ) and  
22

23 275 concentrated ( $c^{**}$ )) as the demarcation lines between these regimes are usually blurred.  
24

25 276 Equation 4 usually describes well the scattering curves of biopolymer chains in homogeneous  
26

27 277 solutions but it fails in the case of solutions with inhomogeneities.<sup>38</sup> In the latter case, a  
28

29 278 second Debye–Bueche term<sup>39</sup> is needed to describe scattering that accounts for the  
30

31 279 correlations within the long-lived entanglements or aggregates.<sup>40</sup> By removing the Guinier  
32

33 280 regime<sup>14</sup> the second term in equation 4 is not required, thus we modelled the scattering from  
34

35 281 the semi-dilute regime fitting data from the power law region between  $\sim 0.03$  and  $0.13 \text{ \AA}^{-1}$ .  
36  
37

38 282 The physical meaning of  $\xi$ , which is particularly affected by electrostatic interactions (e.g.,  
39

40 283 pH, ionic strength),<sup>7</sup> is that at length scales smaller than  $\xi$  most of the monomers in the  
41

42 284 biopolymer chains are surrounded by the solvent or other monomers that belong to the same  
43

44 285 chain whereas at length scales greater than  $\xi$  chains entangle.<sup>15</sup> Estimates of correlation  
45

46 286 lengths at different pH values for both samples compare well with those of other  
47

48 287 polysaccharides (e.g., levan<sup>40,41</sup>, carrageenan or methylcellulose<sup>38</sup>) and reveal an increase in  
49

50 288  $\xi$  with pH for both samples due to electrostatic repulsion that increases the interaction  
51

52 289 distance of the chains.<sup>27</sup> In that case the size of the "mesh" that is formed by the overlapping  
53

54 290 chains increases resulting in a more open structure. Correlation length is greater for sample  
55  
56  
57  
58  
59  
60

1  
2  
3 291 OP6 than OP2 at all pH values. It is possible that the less extensive branching and lower  
4  
5 292 molecular weight of OP2 gives the molecule the chance for more efficient packing thus  
6  
7 293 decreasing the interaction distances. It emerges that a greater  $\zeta$  value has consequences for  
8  
9  
10 294 the functional properties of pectin especially in relation to the interfacial arrangement.  
11  
12 295 Combining information from our previous investigations <sup>42,43</sup> it seems that high  $\zeta$  values  
13  
14 296 correspond to weaker emulsion formation and stabilisation capacity of pectin. This  
15  
16 297 observation is related to the thickness of the adsorbed interfacial layer <sup>44</sup> and the concomitant  
17  
18 298 steric stabilisation.

#### 21 299 4. Conclusions

24 300 The influence of pH on the solution conformation of pectin samples with distinct  
25  
26 301 molecular characteristics and in the presence of 0.1 M NaCl was investigated using small  
27  
28 302 angle X-ray scattering in the dilute and semi-dilute regime of the biopolymers. Irrespectively  
29  
30 303 of the environmental conditions, pectin samples reveal two length scales that are maintained  
31  
32 304 throughout the pH range that was employed (pH 2-7) corresponding to a mass fractal  
33  
34 305 structure with  $d_f$  of about 2 and 1.5 for each length scale, respectively. At acidic pH (pH 2.0)  
35  
36 306 a shift to more compact chain arrangements was observed whereas pH showed little influence  
37  
38 307 at higher pH values (pH 4, 6, 7). Additionally, neutral sugar branches of RG-I moieties  
39  
40 308 contribute to the creation of more compact conformations, irrespectively of the pH of the  
41  
42 309 solvent.

46 310

49 311

52 312

55 313

314 **5. References**

- 315 1. Djabourov, M.; Nishinari, K.; Ross-Murphy, S. B. *Physical Gels from Biological and*  
316 *Synthetic Polymers*; Cambridge University Press: Cambridge, 2013.
- 317 2. Mohnen, D. *Current Opinion in Plant Biology* 2008, 11, 266-277.
- 318 3. Cros, S.; Garnier, C.; Axelos, M. A. V.; Imberty, A.; Perez, S. *Biopolymers* 1996, 39,  
319 339-352.
- 320 4. Ralet, M.-C.; Crepeau, M.-J.; Lefebvre, J.; Mouille, G.; Hofte, H.; Thibault, J.-F.  
321 *Biomacromolecules* 2008, 9, 1454-1460.
- 322 5. Alba, K.; Laws, A. P.; Kontogiorgos, V. *Food Hydrocolloids* 2015, 43, 726-735.
- 323 6. Konarev, P. V.; Volkov, V. V.; Sokolova, A. V.; Koch, M. H. J.; Svergun, D. I.  
324 *Journal of Applied Crystallography* 2003, 36, 1277-1282.
- 325 7. Dobrynin, A. V.; Colby, R. H.; Rubinstein, M. *Macromolecules* 1995, 28, 1859-1871.
- 326 8. Harding, E. S. *Progress in Biophysics and Molecular Biology* 1997, 68, 207-262.
- 327 9. Rinaudo, M. *Structural Chemistry* 2009, 20, 277-289.
- 328 10. Tomsic, M.; Rogac, M. B.; Jamnik, A. *Acta Chimica Slovenica* 2001, 48, 333-342.
- 329 11. Yuguchi, Y.; Tran, V. T. T.; Bui, L. M.; Takebe, S.; Suzuki, S.; Nakajima, N.;  
330 Kitamura, S.; Thanh, T. T. *Carbohydrate Polymers* 2016, 147, 69-78.
- 331 12. Nishida, K.; Kaji, K.; Kanaya, T.; Shibano, T. *Macromolecules* 2002, 35, 4084-4089.
- 332 13. Dror, Y.; Cohen, Y.; Yerushalmi-Rozen, R. *Journal of Polymer Science Part B:*  
333 *Polymer Physics* 2006, 44, 3265-3271.
- 334 14. Josef, E.; Bianco-Peled, H. *Soft Matter* 2012, 8, 9156-9165.
- 335 15. Salamon, K.; Aumiler, D.; Pabst, G.; Vuletic, T. *Macromolecules* 2013, 46, 1107-  
336 1118.
- 337 16. Svergun, D. I.; Koch, M. H. J.; Timmins, P. A.; May, R. P. *Small Angle X-Ray and*  
338 *Neutron Scattering from Solutions of Biological Macromolecules*; Oxford University Press:  
339 Oxford, 2013.
- 340 17. Ventura, I.; Bianco-Peled, H. *Carbohydrate Polymers* 2015, 123, 122-129.
- 341 18. Rambo, R. P.; Tainer, J. A. *Biopolymers* 2011, 95, 559-571.
- 342 19. Bernado, P.; Svergun, D. I. *Molecular BioSystems* 2012, 8, 151-167.
- 343 20. Qazvini, N. T.; Bolisetty, S.; Adamcik, J.; Mezzenga, R. *Biomacromolecules* 2012,  
344 13, 2136-2147.
- 345 21. Gawronski, M.; Conrad, H.; Stahmann, K. P. *Macromolecules* 1996, 29, 7820-7825.
- 346 22. Chivero, P.; Gohtani, S.; Ikeda, S.; Nakamura, A. *Food Hydrocolloids* 2014, 35, 279-  
347 286.
- 348 23. Dogsa, I.; Tomsic, M.; Orehek, J.; Benigar, E.; Jamnik, A.; Stopar, D. *Carbohydrate*  
349 *Polymers* 2014, 111, 492-504.
- 350 24. Dogsa, I.; Kriechbaum, M.; Stopar, D.; Laggner, P. *Biophysical Journal* 2005, 89,  
351 2711-2720.
- 352 25. Morris, G. A.; Ralet, M.-C. *Carbohydrate Polymers* 2012, 88, 1488-1491.
- 353 26. Stokke, B. T.; Draget, K. I.; Smidsrød, O.; Yuguchi, Y.; Urakawa, H.; Kajiwara, K.  
354 *Macromolecules* 2000, 33, 1853-1863.
- 355 27. Yuguchi, Y.; Mimura, M.; Urakawa, H.; Kitamura, S.; Ohno, S.; Kajiwara, K.  
356 *Carbohydrate Polymers* 1996, 30, 83-93.
- 357 28. Muller, F.; Manet, S.; Jean, B.; Chambat, G.; Boue, F.; Heux, L.; Cousin, F.  
358 *Biomacromolecules* 2011, 12, 3330-3336.
- 359 29. Teixeira, J. *Journal of Applied Crystallography* 1988, 21, 781-785.
- 360 30. Beaucage, G. *Journal of Applied Crystallography* 1996, 29, 134-146.

- 1  
2  
3 361 31. Georgiades, P.; di Cola, E.; Heenan, R. K.; Pudney, P. D. A.; Thornton, D. J.; Waigh,  
4 362 T. A. *Biopolymers* 2014, 101, 1154-1164.  
5 363 32. Mansel, B. W.; Chu, C.-Y.; Leis, A.; Hemar, Y.; Chen, H.-L.; Lundin, L.; Williams,  
6 364 M. A. K. *Biomacromolecules* 2015, 16, 3209-3216.  
7 365 33. Putnam, C. D.; Hammel, M.; Hura, G. L.; Tainer, J. A. *Quarterly Reviews of*  
8 366 *Biophysics* 2007, 40, 191-285.  
9 367 34. Kirby, A. R.; MacDougall, A. J.; Morris, V. J. *Carbohydrate Polymers* 2008, 71, 640-  
10 368 647.  
11 369 35. Tombs, M. P.; Harding, S. E. *An introduction to polysaccharide biotechnology*;  
12 370 Taylor and Francis: London, 1998.  
13 371 36. Morris, G. A.; de al Torre, J. G.; Ortega, A.; Castile, J.; Smith, A.; Harding, S. E.  
14 372 *Food Hydrocolloids* 2008, 22, 1435-1442.  
15 373 37. Yukioka, S.; Higo, Y.; Noda, I.; Nagasawa, M. *Polym J* 1986, 18, 941-946.  
16 374 38. Cerar, J.; Jamnik, A.; Tomšič, M. *Acta Chimica Slovenica* 2015, 62.  
17 375 39. Debye, P.; Bueche, A. M. *Journal of Applied Physics* 1949, 20, 518-525.  
18 376 40. Benigar, E.; Dogsa, I.; Stopar, D.; Jamnik, A.; Cigić, I. K.; Tomšič, M. *Langmuir*  
19 377 2014, 30, 4172-4182.  
20 378 41. Benigar, E.; Zupančič Valant, A.; Dogsa, I.; Sretenovic, S.; Stopar, D.; Jamnik, A.;  
21 379 Tomšič, M. *Langmuir* 2016, 32, 8182-8194.  
22 380 42. Alba, K.; Sagis, L. M. C.; Kontogiorgos, V. *Colloids and Surfaces B: Biointerfaces*  
23 381 2016, 145, 301-308.  
24 382 43. Alba, K.; Kontogiorgos, V. *Food Hydrocolloids* 2016, doi:  
25 383 10.1016/j.foodhyd.2016.1007.1026.  
26 384 44. Dobrynin, A. V.; Rubinstein, M. *Progress in Polymer Science* 2005, 30, 1049-1118.

385

386

387

388

389

390

391

392

393

394



395 **FIGURE LEGENDS**

396 **Figure 1:** Schematic representation of major pectin building blocks primarily responsible for  
397 conformational characteristics of pectin in solution. HG is the homogalacturonan and RG-I is  
398 the rhamnogalacturonan-I regions.

399 **Figure 2:** Small-angle X-ray scattering intensity plots of OP2 pectin samples at all pH values  
400 in the presence of 0.1 M NaCl in the (a) dilute and (b) semi-dilute regime of the biopolymer.  
401 Top right inset shows how the cross-sectional radius of gyration was calculated from  $\ln(I)$  vs.  
402  $q^2$  plots. Bottom right inset shows scattering intensity plots of sample OP6 at the semi-dilute  
403 regime.

404 **Figure 3:** Kratky plots of samples of OP2 samples in the (a) dilute and (b) semi-dilute regime  
405 of the biopolymers. A peak at about  $0.07 \text{ \AA}^{-1}$  followed by a sharp decay before starting  
406 increasing again at  $0.15 \text{ \AA}^{-1}$  indicates partially folded chains with elongated domains  
407 corresponding to multi-domain particles.

408 **Figure 4:** Porod plots of (a) OP6 in the dilute and (b) OP2 in the semi-dilute regime of the  
409 biopolymers with a transition occurring at  $0.08 \text{ \AA}^{-1}$ . Slopes are also shown for each region.

410

411

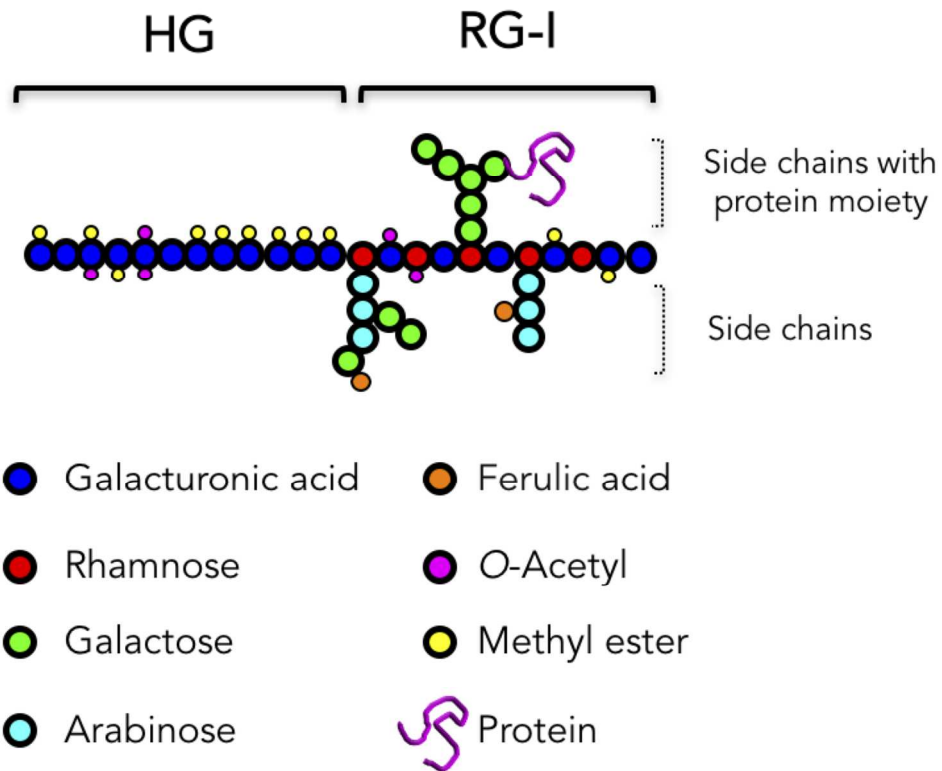
412

413

**Table 1:** Molecular characteristics of samples obtained from SAXS data analysis.

		$R_c$ (Å)	Slope 1	Slope 2	$l_o$ (Å)	$\xi$ (Å) <sup>a</sup>
	<b>pH 2</b>	12	-1.8	-1.0	42	-
<b>OP2 Dilute</b>	<b>pH 4</b>	15	-1.9	-1.5	52	-
	<b>pH 6</b>	15	-2.0	-1.3	52	-
	<b>pH 7</b>	20	-1.5	-1.4	69	-
<b>OP2 Semi dilute</b>	<b>pH 2</b>	15	-1.8	-1.4	52	32 (0.962)
	<b>pH 4</b>	16	-1.9	-1.8	55	50 (0.950)
	<b>pH 6</b>	16	-1.9	-1.8	55	55 (0.932)
	<b>pH 7</b>	21	-2.0	-1.8	73	97 (0.876)
<b>OP6 Dilute</b>	<b>pH 2</b>	11	-2.1	-1.0	38	-
	<b>pH 4</b>	17	-2.0	-1.5	59	-
	<b>pH 6</b>	20	-2.0	-1.5	69	-
	<b>pH 7</b>	24	-1.5	-1.6	83	-
<b>OP6 Semi dilute</b>	<b>pH 2</b>	19	-2.3	-1.5	66	65 (0.925)
	<b>pH 4</b>	20	-2.1	-1.7	69	102 (0.960)
	<b>pH 6</b>	21	-2.2	-1.8	73	106 (0.904)
	<b>pH 7</b>	23	-2.1	-1.8	80	154 (0.824)

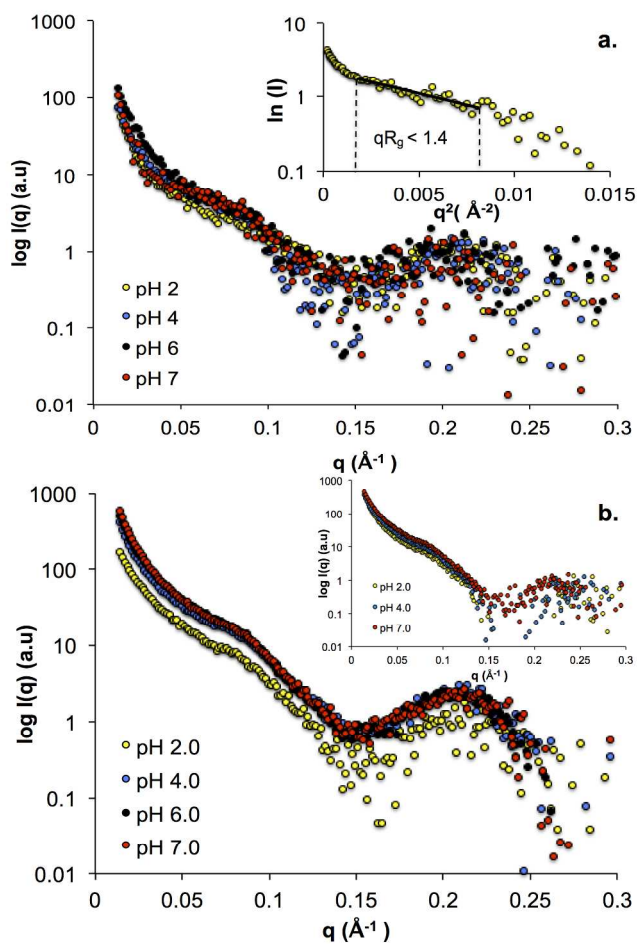
a: Value in the brackets shows the  $r^2$  of fitting the Ornstein-Zernike relationship to the SAXS data



Schematic representation of major pectin building blocks primarily responsible for conformational characteristics of pectin in solution. HG is the homogalacturonan and RG-I is the rhamnogalacturonan-I regions.

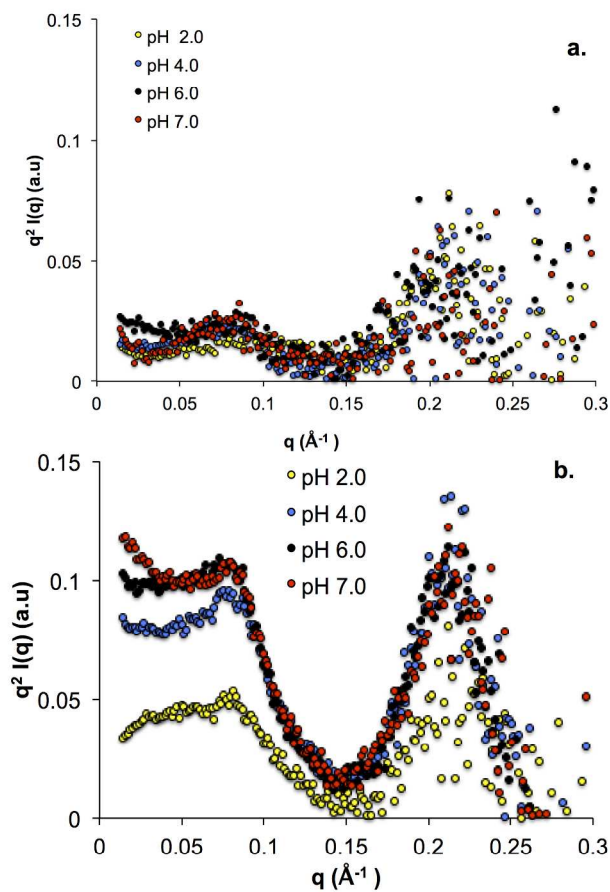
128x105mm (300 x 300 DPI)

1  
2  
3  
4  
5  
6  
7  
8  
9  
10  
11  
12  
13  
14  
15  
16  
17  
18  
19  
20  
21  
22  
23  
24  
25  
26  
27  
28  
29  
30  
31  
32  
33  
34  
35  
36  
37  
38  
39  
40  
41  
42  
43  
44  
45  
46  
47  
48  
49  
50  
51  
52  
53  
54  
55  
56  
57  
58  
59  
60



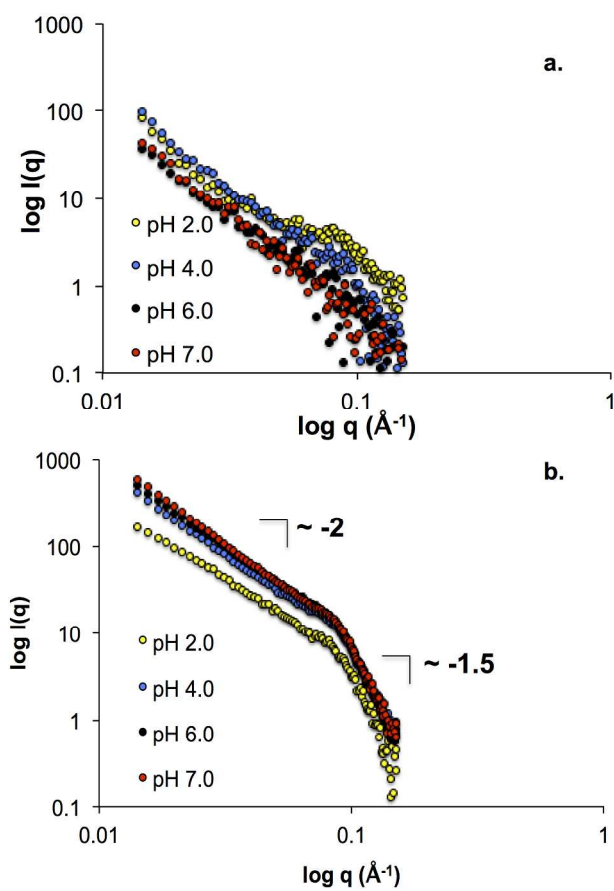
Small-angle X-ray scattering intensity plots of OP2 pectin samples at all pH values in the presence of 0.1 M NaCl in the (a) dilute and (b) semi-dilute regime of the biopolymer. Top right inset shows how the cross-sectional radius of gyration was calculated from  $\ln(I)$  vs.  $q^2$  plots. Bottom right inset shows scattering intensity plots of sample OP6 at the semi-dilute regime.

215x279mm (300 x 300 DPI)



Kratky plots of samples of OP2 samples in the (a) dilute and (b) semi-dilute regime of the biopolymers. A peak at about  $0.07 \text{\AA}^{-1}$  followed by a sharp decay before starting increasing again at  $0.15 \text{\AA}^{-1}$  indicates partially folded chains with elongated domains corresponding to multi-domain particles.

215x279mm (300 x 300 DPI)



Porod plots of (a) OP6 in the dilute and (b) OP2 in the semi-dilute regime of the biopolymers with a transition occurring at  $0.08 \text{\AA}^{-1}$ . Slopes are also shown for each region.

215x279mm (300 x 300 DPI)